

# Quantitative Proteomic Analysis of the Adipocyte Plasma Membrane

Matthew J. Prior,<sup>†,‡</sup> Mark Larance,<sup>†,‡</sup> Robert T. Lawrence,<sup>†,‡</sup> Jamie Soul,<sup>†</sup> Sean Humphrey,<sup>†</sup> James Burchfield,<sup>†</sup> Carol Kistler,<sup>§</sup> Jonathon R. Davey,<sup>†</sup> Penelope J. La-Borde,<sup>†</sup> Michael Buckley,<sup>||</sup> Hiroshi Kanazawa,<sup>⊥</sup> Robert G. Parton,<sup>§</sup> Michael Guilhaus,<sup>#,¶</sup> and David E. James<sup>\*,†</sup>

<sup>†</sup>Diabetes and Obesity Program, Garvan Institute of Medical Research, Sydney, NSW 2010, Australia

<sup>§</sup>Institute for Molecular Bioscience, University of Queensland, Queensland 4072, Brisbane, Australia

<sup>||</sup>CSIRO Mathematics, Informatics and Statistics, Locked Bag 17, North Ryde, NSW 2113, Australia

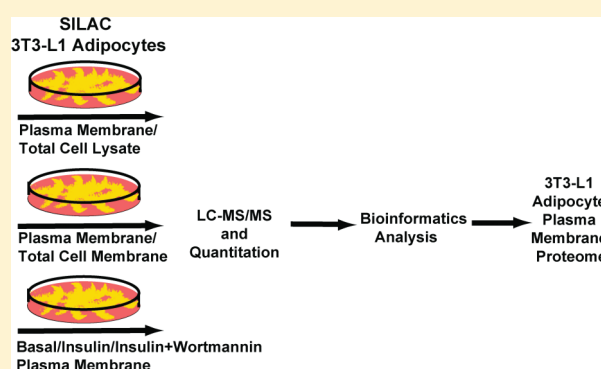
<sup>⊥</sup>Department of Biological Science, Osaka University, Machikaneyama, Toyonaka, Osaka 560-0043, Japan

<sup>#</sup>Bioanalytical Mass Spectrometry Facility, University of New South Wales, Sydney, NSW 2052, Australia

**S** Supporting Information

**ABSTRACT:** The adipocyte is a key regulator of mammalian metabolism. To advance our understanding of this important cell, we have used quantitative proteomics to define the protein composition of the adipocyte plasma membrane (PM) in the presence and absence of insulin. Using this approach, we have identified a high confidence list of 486 PM proteins, 52 of which potentially represent novel cell surface proteins, including a member of the adiponectin receptor family and an unusually high number of hydrolases with no known function. Several novel insulin-responsive proteins including the sodium/hydrogen exchanger, NHE6 and the collagens III and VI were also identified, and we provide evidence of PM-ER association suggestive of a unique functional association between these two organelles in the adipocyte. Together these studies provide a wealth of potential therapeutic targets for the manipulation of adipocyte function and a valuable resource for metabolic research and PM biology.

**KEYWORDS:** proteomics, GLUT4, insulin action, NHE6, SILAC, plasma membrane, 3T3-L1 adipocyte



## INTRODUCTION

The plasma membrane (PM) represents a selective filter for the transmission of molecules and information between the internal and external cellular environments. The PM achieves this through the expression of a range of proteins with varying biological functions, including receptors that bind extracellular ligands and transmit signals via signal transduction cascades, channels, and transporters which physically move small molecules such as sugars or ions across the membrane and structural proteins that regulate cell shape, motility, or rigidity. While the functional identity of organelles such as the PM can be defined by their protein composition, it has become apparent that many proteins do not permanently reside in such compartments. Instead, there is a dynamic flux of proteins between organelles as the cell interacts with its surroundings.

The adipocyte plays a key role in insulin-regulated glucose and lipid metabolism and thus has been implicated in the development of insulin resistance and metabolic disease.<sup>1</sup> The actions of insulin in the adipocyte are mediated through the insulin receptor on the PM. Activation of the tyrosine kinase activity of this receptor following insulin binding leads to the generation of phosphatidylinositol-3,4,5-triphosphate in the PM inner leaflet and the subsequent recruitment of various signaling molecules

such as phosphoinositide-dependent protein kinases and Akt, to the PM.<sup>2</sup> Akt activation results in major modifications in the composition of the PM exemplified by the transient increase in the amount of the insulin-responsive glucose transporter, GLUT4 at the cell surface;<sup>3</sup> a response that is impaired in patients with Type 2 Diabetes.<sup>4,5</sup> Thus, defining the protein composition of the PM under a range of metabolic conditions and in response to a range of external challenges will improve our understanding of the functions mediated by a particular cell type and yield a list of novel targets for the therapeutic manipulation of those functions.

To this end, we conducted a comprehensive global proteomic analysis of the adipocyte PM both before and after acute insulin stimulation. We used cationic colloidal silica to isolate the PM from 3T3-L1 adipocytes combined with stable isotope labeling with amino acids in cell culture (SILAC) for quantitative analysis using mass spectrometry.<sup>6</sup> We also combined these approaches with the use of Gene Ontology (GO) cellular compartment annotations to identify a high confidence list of adipocyte PM proteins. Together, these studies provide a greater understanding

**Received:** May 15, 2011

**Published:** September 19, 2011

of the signaling architecture within the adipocyte and provide novel insights into the cell biology of the PM.

## MATERIALS AND METHODS

### Materials

3T3-L1 murine fibroblasts were purchased from the American Type Culture Collection (ATCC, Rockville, MD). Dulbecco's Modified Eagle Medium (DMEM) was obtained from Invitrogen (Carlsbad, CA) and myoclonal-plus fetal calf serum (FCS) from Trace Scientific (Melbourne, Australia). Bovine insulin was obtained from Calbiochem (San Diego, CA) and bovine serum albumin (BSA) from USB (Cleveland, OH). Bicinchoninic acid (BCA) reagent, GF-2000 beads and Supersignal West Pico chemiluminescent substrate were from Pierce (Rockford, IL). C18 cartridges were from Michrom (Auburn, CA). Magic C18 material was from Alltech (Deerfield, IL). Complete protease inhibitor cocktail tablets were from Roche (Indianapolis, IN). Poly(acrylic acid) partial sodium salt solution (average  $M_w$  approximately 240 000) and all other materials were obtained from Sigma (St. Louis, MO). The KDEL-HRP construct was a kind gift from Professor Colin Hopkins, Imperial College, London<sup>7</sup> and antibodies were kindly provided by Dr. Wanjin Hong (Syntaxin 16, IMCB, Singapore) and Professor Hiroshi Kanazawa (NHE6, Osaka University, Japan). Antibodies were purchased from Santa Cruz Biotechnology (Pan 14-3-3 and Col6a1), BD Biosciences (Caveolin 1), Enzo Life Sciences (Calnexin), Cell Signaling (VDAC) and Sigma-Aldrich ( $\beta$ -actin). Antibodies against GLUT4, IRAP and Syntaxin-4 have been described previously.<sup>8</sup> Cy5 and Cy3-conjugated secondary antibodies were obtained from Jackson ImmunoResearch (West Grove, PA). Alexa Fluor 680-conjugated secondary antibodies were obtained from Invitrogen. IrDye 800-conjugated secondary antibodies were obtained from Rockland Immunochemicals (Gilbertsville, PA). HRP-conjugated secondary antibodies were from GE Healthcare (Buckinghamshire, U.K.).

### Cell Culture

3T3-L1 fibroblasts were cultured in Dulbecco's modified Eagle's medium (DMEM) supplemented with 10% fetal calf serum, 2 mM L-glutamine, 100 units/L penicillin, and 100 g/L streptomycin at 37 °C in 10% CO<sub>2</sub>. SILAC labeled and unlabeled 3T3-L1 fibroblasts were differentiated as previously described by the addition of isobutyl-1-methyl-xanthine (IBMX, 500  $\mu$ M), dexamethasone (0.22  $\mu$ M), insulin (0.35  $\mu$ M) and biotin (409 nM) to confluent cells for 3 days, followed by 3 days of post differentiation in growth media plus insulin (0.35  $\mu$ M).<sup>9</sup> Adipocytes were maintained in growth media and used between days 8 and 10 postdifferentiation and between passages 10 and 20. For triple and double SILAC labeling of 3T3-L1 adipocytes arginine and lysine free DMEM (Sigma) was supplemented with either unlabeled arginine (21 mg/L) and lysine (36.4 mg/L) ("light"), <sup>13</sup>C<sub>6</sub>-arginine (21.6 mg/L) and <sup>2</sup>H<sub>4</sub>-lysine (44.5 mg/L) ("medium") (Silantes, GmbH) or <sup>13</sup>C<sub>6</sub>-<sup>15</sup>N<sub>4</sub>-arginine (22.0 mg/L) and <sup>13</sup>C<sub>6</sub>-<sup>15</sup>N<sub>2</sub>-lysine (38.0 mg/L) ("heavy") (Silantes, GmbH) as described previously.<sup>10</sup>

### Cationic Colloidal Silica Isolation of Associated and Integral PM Proteins

PM was purified as per Chaney and Jacobson with modifications.<sup>11</sup> Briefly, 3–4 10 cm dishes of 3T3-L1 adipocytes per condition were washed twice with ice-cold PBS and twice in ice-cold coating buffer (20 mM MES, 150 mM NaCl, 280 mM sorbitol, pH 5.0–5.5). Adipocytes were coated with 1% (w/v) cationic colloidal silica (a kind gift from Associate Professor D. Beer Stolz,

(University of Pittsburgh) and prepared as previously described<sup>11</sup>) in coating buffer for 2 min on ice. Excess silica was removed by washing once with ice-cold coating buffer. Poly(acrylic acid) partial sodium salt (1 mg/mL, pH 6–6.5) was added to the cells in coating buffer and incubated at 4 °C for 2 min. Cells were washed in ice-cold coating buffer, followed by modified HES (20 mM HEPES, 250 mM sucrose, 1 mM dithiothreitol, 1 mM magnesium acetate, 100 mM potassium acetate, 0.5 mM zinc chloride, pH 7.4) at 4 °C and lysed using 12 passes through a 22-G needle followed by 6 passes through a 27-G needle in modified HES buffer containing complete protease inhibitors (Roche) and phosphatase inhibitors (2 mM sodium orthovanadate, 1 mM pyrophosphate, 1 mM ammonium molybdate, 10 mM sodium fluoride) at 4 °C. Nycodenz (100%) in modified HES buffer was added to a final concentration of 50% and layered onto 1.5 mL 70% Nycodenz in modified HES and centrifuged in a swing-out rotor at 41 545 $\times$  g for 20 min at 4 °C. The supernatant was discarded, and the pellet was washed several times in modified HES buffer. To obtain the associated membrane fraction, the pellet was resuspended in a high pH and high salt solution (1 M NaCl and 100 mM Na<sub>2</sub>CO<sub>3</sub>, pH 11.0–11.5).<sup>12</sup> This mixture was centrifuged at 500 $\times$  g for 5 min at 4 °C and the supernatant was collected and centrifuged at 100 000 $\times$  g for 1 h at 4 °C. The supernatant from this spin was retained for SDS-PAGE analysis and routinely contained between 50 and 100  $\mu$ g protein per dish used. The pellet from the high pH, high salt wash (approximately 75  $\mu$ g/10 cm dish used), containing the integral membrane proteins was resuspended in RIPA buffer (50 mM Tris-Cl pH 7.4, 150 mM NaCl, 1% NP-40, 0.5% sodium deoxycholate, 0.1% SDS), containing protease and phosphatase inhibitors and centrifuged at 500 $\times$  g for 5 min at 4 °C to remove the silica beads.

### Insulin and Wortmannin Treatments

To establish basal conditions, SILAC or unlabeled adipocytes were serum starved for 3 h at 37 °C in 10% CO<sub>2</sub>. For SILAC experiments, cationic silica PM fractions were isolated from 3T3-L1 adipocytes, which were serum starved (light), stimulated with 100 nM insulin for 20 min (medium) or exposed to 100 nM wortmannin for 20 min prior to insulin stimulation (heavy). Lysate protein content was determined by BCA assay for each SILAC label and lysates were mixed in a 1:1:1 ratio prior to the addition of Nycodenz (100%) during PM isolation by cationic colloidal silica.

### Subcellular Fractionation of Adipocytes and SILAC PM Enrichment Analysis

3T3-L1 adipocyte fractionation and total cell membrane preparations were carried out as described previously<sup>9</sup> using 1–2 10 cm dishes of cells per condition. For SILAC, PM enrichment analysis, adipocytes were serum starved for 2–3 h prior to fractionation or lysis and 10  $\mu$ g of whole cell lysate in RIPA buffer (3 mg protein/10 cm dish - medium) was combined with 10  $\mu$ g cationic silica associated PM (50–100  $\mu$ g protein/10 cm dish - light) or integral PM (50–100  $\mu$ g protein/10 cm dish - light). Total cell membrane (10  $\mu$ g) in RIPA buffer (500–800  $\mu$ g/10 cm dish - light) was combined with 10  $\mu$ g cationic silica PM (100–200  $\mu$ g/10 cm dish - medium). All protein mixtures were resolved on 10% acrylamide gels prior to LC-MS/MS analysis.

### GLUT4 Vesicle Immunoadsorption

GLUT4 vesicles were immunoadsorbed from low density microsome (LDM) fractions using control mouse IgG or anti-GLUT4

monoclonal 1F8 covalently coupled to GF-2000 beads, as previously described.<sup>8</sup>

### Tissue Distribution and Lysate Preparation

Tissues were collected and processed as previously described<sup>13</sup> with the approval of the Garvan Institute/St.Vincent's Hospital Animal Experimentation Ethics Committee following guidelines issued by the National Health and Medical Research Council (NHMRC) of Australia. Following homogenization, all tissue and cell lysates were centrifuged at  $16\,000\times g$  for 15 min at 4 °C. Supernatant protein concentration was determined by the BCA assay.

### SDS-PAGE and Immunoblotting

Samples (10–20 µg protein) were resolved by SDS-PAGE on 10% polyacrylamide gels for mass spectrometry and immunoblotting analysis. For mass spectrometry, gels were stained using SYPRO Ruby (Molecular Probes). Western blotting was performed as previously described.<sup>8</sup>

### In-gel Protein Tryptic Digestion, LC–MS/MS, Identification and Quantitation

In gel protein tryptic digestion was performed as described.<sup>14</sup> For LC–MS/MS analysis, peptide solutions (5 µL) were separated on a 12 cm 75 µM ID analytical column pulled to an internal diameter of 5 µM by a P-2000 laser puller (Sutter Instruments Co) and packed with C18 Magic reverse phase material using a Dionex Ultimate 3000 LC system. Peptides were separated over a gradient of 1–3 h at a flow rate of 200 nL/min and electrosprayed directly into the mass spectrometer using a spray voltage of 1.8 kV. Mass spectrometry was performed using a Thermo Fisher Scientific (San Jose, CA) LTQ-FT Ultra mass spectrometer. The data-dependent acquisition method used was the FT10 protocol, described previously.<sup>15</sup> Data were processed, searched and quantified using the MaxQuant software version 1.0.13.13 package as described previously<sup>16</sup> using default settings, with the following variable modifications: oxidized methionine (M) and propionamide cysteine (C) as cysteine residues were not blocked experimentally prior to SDS-PAGE analysis. Searches were performed using Mascot server version 2.2 against the mouse IPI database (version 3.71). Using the default MaxQuant settings a false discovery rate (FDR) threshold of 1% is specified at the peptide and protein level. Protein quantitation data was always derived from two or more peptides per protein of which at least one of which must be unique. For all SILAC experiments, ratios were deemed significantly different from 1 when they reached a significance level of (B) <0.05 using the MaxQuant software.<sup>16</sup> All raw mass spectrometry data from technical replicates were combined and analyzed together using the MaxQuant software. Biological replicates were analyzed separately and the mean and standard deviation calculated for each protein identified from these replicates. The raw mass spectrometry data associated with this manuscript may be downloaded from ProteomeCommons.org Tranche using the following hash: 8W6p1KCAl6W58wEF44xaNq/Xg0qGhuKfLLCYT3p8k9m-CBMO/WxCGs8tlre1DQO8mtES/rvK+OdoITNiNNonfyNO-hqjIAAAAAA5Kw==.

### Immunofluorescence and Electron Microscopy

For visualization of the ER in 3T3-L1 adipocytes by EM, KDEL-HRP was expressed in differentiated 3T3-L1 adipocytes by electroporation according to standard methods.<sup>17</sup> Fixation, visualization of the HRP reaction product, and further processing for Epon embedding was according to standard procedures.

Sections were cut parallel to the substratum. For immunofluorescence microscopy, cells were fixed with 3.8% paraformaldehyde in PBS, washed with PBS, quenched with 50 mM glycine in PBS and permeabilised in PBS containing 0.1% saponin and 2% BSA. Primary antibodies were detected with Cy3 or Cy2 conjugated secondary antibodies. Optical sections were analyzed by epifluorescence microscopy on a Leica SP2 inverted confocal microscope. Images were generated from a single slice of a z-stack taken from the top to the bottom of the cell monolayer. Human ASCT2 (SLC1A5) in pEGFP-N1 (Clontech) or human Rab35 in pTagRFP-C Gateway, constructed by inserting the Gateway cassette B into the *SmaI* site of pTagRFP-C (Evrogen) was electroporated into differentiated 3T3-L1 adipocytes as described above.

### Bioinformatic and Statistical Analysis

IPI identifiers were mapped to Gene Ontology Cellular Components (GOCC) and to the Panther classification system using the DAVID bioinformatics database.<sup>18</sup> Analysis of statistical over- or under-representation of available ontologies was performed using the algorithms provided in DAVID. For all enrichment analysis, proteins were categorized as either PM, ER, mitochondria, nuclear, cytoplasmic, golgi or other using GOCC annotations. GOCC annotation strings were initially searched for the terms “plasma membrane”, “extracellular matrix”, “extracellular region”, “extracellular space”, “cell periphery” and “cell surface”. Proteins with one or more of these annotations were classified as PM. Annotations for all remaining proteins were searched for terms “endoplasmic reticulum”, “Golgi”, “mitochondrion” (or “mitochondrial”), and “nucleus” (or “nuclear”) and the protein was classified accordingly if only one of these terms matched. Remaining proteins were classified as cytoplasm if the initial GOCC field was “cytoplasm”, or as “other”. PM protein lists were manually curated using The Human Protein Atlas (<http://www.proteinatlas.org/>) in combination with literature searches using PubMed (<http://www.ncbi.nlm.nih.gov/pubmed>). Only proteins exhibiting evidence of PM localization in both were classified as *bona fide* PM proteins. The total mouse ER data set was obtained from the GO database (<http://www.geneontology.org/>) and transmembrane domains and secreted proteins were predicted using the TMHMM algorithm,<sup>19</sup> as previously described.<sup>20</sup> Protein sequence analysis was performed using InterProScan Sequence Search using default settings<sup>21</sup> and functional annotations were assigned using literature searches of the PubMed database. Statistical calculations were done using the statistical environment, R.<sup>22</sup> Mixture modeling was done using the package “mclust”.<sup>23</sup>

## RESULTS

### Isolation of Adipocyte PM Fractions

To capture PM enriched proteins, several different subcellular fractionation methods were trialed including differential centrifugation and cationic silica labeling as described previously.<sup>9,11</sup> Consistent with our previous findings,<sup>8</sup> the cationic silica method was found to be optimal because it isolates a PM fraction more highly enriched in PM markers such as caveolin 1 and syntaxin 4 but less enriched in the Golgi marker syntaxin 16 and the mitochondrial marker VDAC (Figure 1A) than other traditional methods. Furthermore, the procedure is rapid and of sufficiently low stringency to preserve peripheral associations.<sup>8,11</sup> Additional reductions in sample complexity for LC–MS/MS analysis were attained through further fractionation of the cationic silica PM

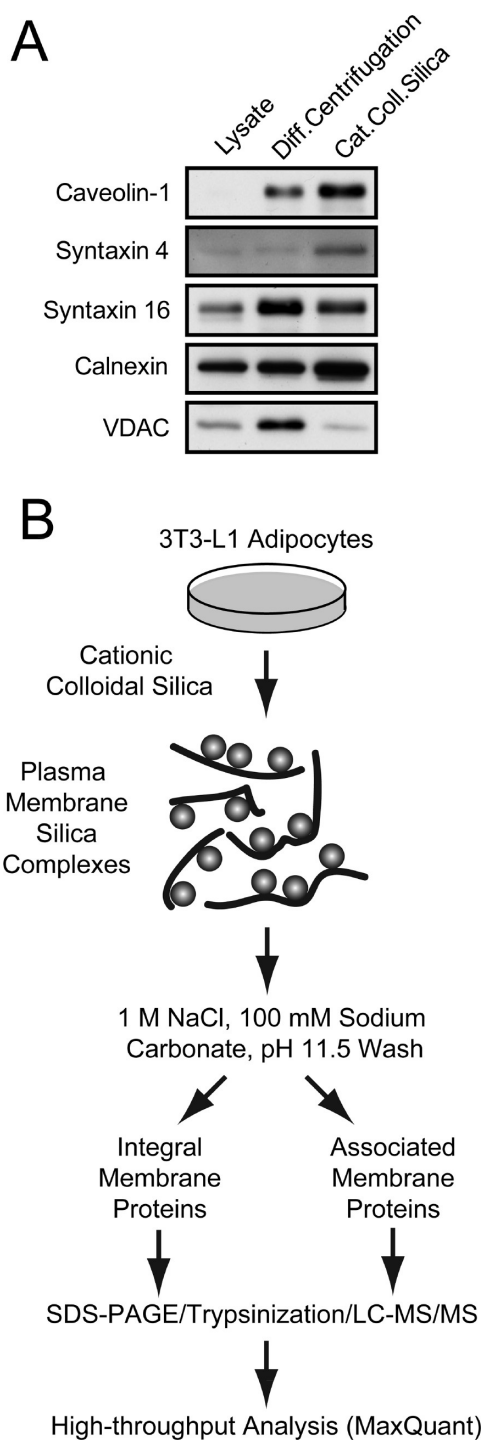


**Figure 1.** (A) Comparison of organelle constituents found in the differential centrifugation and cationic colloidal silica PM fractions. Equal amounts of 3T3-L1 protein lysate and PM were immunoblotted using the PM, Golgi, ER and mitochondrial markers listed. The experiment was performed two times and the images are from a representative experiment. (B) Outline of the materials and methods utilized to survey the 3T3-L1 PM proteome. PM protein fractions obtained by cationic colloidal silica were subfractionated into integral and associated PM proteins using a high salt, high pH wash. Proteins were subjected to LC-MS/MS and the output analyzed using MaxQuant software (Table S1, Supporting Information). See also Supplementaery Figure S1 (Supporting Information).

preparation into integral and associated proteins (Figure 1B; Supplemental Figure S1A–C, Supporting Information).

### Identification of the Adipocyte PM Proteome

LC-MS/MS analysis of the cationic silica fraction isolated from adipocytes identified 2600 proteins (Supplemental Table S1, Supporting Information). In combination with a previous study describing MS analysis of the entire adipocyte,<sup>24</sup> this represents one of the largest and most comprehensive proteomic analyses of this cell type. Further analysis of our data using the GO database,<sup>25</sup> however, revealed that many proteins found in the cationic silica fraction were annotated as constituents of alternate organelles, such as mitochondria (22.8%), endoplasmic reticulum (ER) (12.3%) and Golgi (6.0%) (Supplemental Figure S1D; Supplemental Table S1, Supporting Information). This suggests that the proteins from these organelles can also be found at the PM, or alternatively, that our PM cationic silica fraction contains a large proportion of contaminating proteins from other organelles.

The limitation of the GO analysis described above is that it does not provide a quantitative assessment of the relative enrichment of different proteins in the PM fraction. To circumvent this and refine the identification of PM proteins from our cationic silica PM fraction, we employed SILAC to measure the relative enrichment of proteins in the integral and associated cationic silica PM fractions relative to the whole cell lysate (Figure 2). Similar methods have been used to study the centrosomal,<sup>26</sup> mitochondrial<sup>27</sup> and peroxisome proteomes<sup>28</sup> and the cells were serum starved prior to lysis or fractionation for us to more easily compare the resulting proteome with that from our insulin treatments which were performed in the absence of serum. We reasoned that this would enable us to distinguish *bona fide* PM proteins from contaminants in that those proteins with a high PM/whole cell lysate enrichment ratio, similar to that of a GO annotated PM protein, are more likely to be associated with the PM than those proteins with a lower ratio. This resulted in the combined identification of 1528 proteins from the cationic silica integral (Supplemental Table S2, Supporting Information) and associated PM fractions (Supplemental Table S3, Supporting Information).

A broad range of PM cationic silica:lysate Log<sub>2</sub> ratios (7-fold to –5-fold) was observed in both the integral and associated PM fractions. We next wanted to determine if those proteins with the highest ratio represented true PM proteins and if we could use this method to begin to identify nonannotated PM proteins. This proved to be the case for the cationic silica integral PM protein fraction, with proteins predicted to be in the PM, based on GO analysis, found in the rightward population of the frequency distribution, while proteins of other origin, with the exception of ER, were found in the population to the left of the distribution (Figure 3A). Modeling of these data (Figure 3A) indicated that the proteins identified, segregated into two distinct populations with statistically different means, allowing us to separate the two populations. Using a 1% false positive rate (FPR) cut off, 511 proteins were selected from the right-hand curve of the fitted mixture in Figure 3A (Supplemental Table S2, Supporting Information). This population was enriched in PM (1.7-fold) and ER (2.2-fold) annotated proteins relative to the entire data set, but contained 73.5, 45.2, 92.0 and 91.2% fewer mitochondrial, Golgi, nuclear and cytoplasmic-annotated proteins, respectively (Figure 3B).

A similar analysis was performed using the associated cationic silica PM fraction, resulting in the selection of 473 proteins

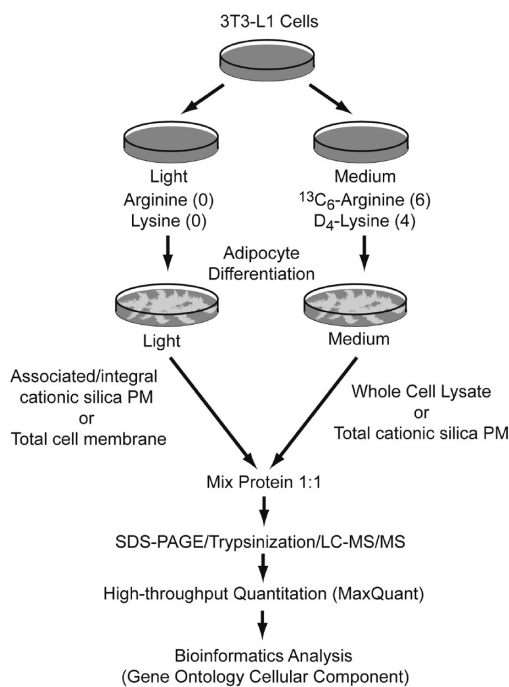


**Figure 2.** Experimental scheme for double SILAC labeling of 3T3-L1 adipocytes for the relative enrichment analysis of the cationic silica PM fraction from whole cell lysate and total cell membrane. Double SILAC labeled 3T3-L1 fibroblasts were differentiated into adipocytes and serum-starved for 2–3 h. Equal protein amounts of whole cell lysate (medium label) was mixed with integral PM (light label) or associated PM (light label). The protein mixtures were then subsequently separated by SDS-PAGE and the entire gel lane digested with trypsin and analyzed by LC–MS/MS. Raw mass spectrometry data was analyzed by the MaxQuant software program. The isotopic labels were swapped for the relative enrichment analysis of total PM (associated and integral) (medium label) from total cell membrane (light label).

(Figure 2; Figure 3C; Supplemental Table S3, Supporting Information). Despite an 86.7% reduction in the number of mitochondrial proteins present in this population relative to the entire data set, there was no enrichment of PM or ER proteins in this data set but a reasonable enrichment of nuclear proteins was observed (1.7-fold) (Figure 3D; Supplemental Table S3, Supporting Information). Given the enrichment of nuclear and ER proteins in the associated and integral PM cationic silica fractions, respectively, we repeated the above analysis using a total cell membrane fraction instead of whole cell lysate, to further assess the purity of our cationic silica PM fraction (Figure 2). Over 2100 proteins were quantitated in the cationic silica PM and total cell membrane fractions (Supplemental Table S4, Supporting Information). Again, the data segregated into two statistically distinct populations (Figure 3E), which were separated by mixture modeling using a 1% FPR. This yielded a list of 549 proteins (Supplemental Table S4, Supporting Information) enriched in PM (1.7-fold) and ER (2.8-fold) proteins relative to the entire data set but reduced in the proportion of mitochondrial (97.7%), Golgi (87.3%) and cytoplasmic (83.7%) proteins (Figure 3F), as previously observed. This indicates that our cationic silica PM fraction is not simply a composite of whole cell membranes further illustrating the use of this enrichment procedure for the identification of high confidence PM proteins.

### Characterization of the Adipocyte PM Proteome

We next manually curated the data to annotate the proteins found in the upper population from each of the enrichment experiments described above. This was an essential step as a number of mis-annotations have previously been identified in GO<sup>29</sup> and it also enabled us to segregate ER proteins from the list. Using this approach we generated a high confidence list of adipocyte PM proteins comprising 486 proteins (Supplemental Table S5, Supporting Information). This list contained many *bona fide* PM proteins, including the Na<sup>+</sup>/K<sup>+</sup> ATPase, Syntaxin 4 and the insulin receptor. Further analysis (see “Materials and Methods”) of this compendium, lead to the identification of 191 proteins (39.3%) with at least one predicted transmembrane (TM) domain and 24 (4.9%) predicted secreted proteins. After filtering out secreted proteins, 34.4% (167 proteins) of remaining proteins were predicted to be integral PM proteins. Of these, 10.7% (52 proteins) have no previous PM annotation and include PAQR4, TMTC3, ATP13A and ABHD1 as well as a suite of TMEM proteins. A further 0.6% (3 proteins) of these TM proteins, including DCAKD and the protein homologues C9orf5 and C6orf64, have no subcellular annotation at all and thus potentially represent novel pharmacological targets. To further validate this procedure we selected Rab35 and ASCT2 (SLC1A5), two proteins identified in our screen, and experimentally examined their localization. As shown in Supplemental Figure S2 (Supporting Information), both RFP-Rab35 and ASCT2-GFP were almost exclusively localized to the cell surface of the adipocyte by immunofluorescence microscopy.

The adipocyte PM proteome identified here, comprises proteins from several functional groups as determined by ontological classification (Table 1 and Supplemental Table S5, Supporting Information). As expected, a large number of cytoskeletal proteins (47), transporters (38), membrane traffic proteins (36), small GTPases (26) and cell adhesion molecules (23) were observed and SNAREs (21%), G-proteins (15%) and in particular heterotrimeric G-proteins (27%), were significantly enriched in our adipocyte PM proteome, indicative of a generic role in membrane function. A large number of receptors (32) and kinases (23) were also observed in the adipocyte PM. In contrast to that observed for many of the other protein families (see above), this represents a relatively small proportion of the total cohort of these kinds of proteins found in the genome, consistent with the view that receptors and kinases play an important role in defining cellular specificity. The proteome is also comprised of a large number of proteins (24) with no functional or subcellular annotation, including FUNDC2, BZW1 and 2 and MIOS to name a few and thus these findings, together with additional bioinformatic analyses, provide vital functional information about each of these uncharacterised proteins (Supplemental Table S6, Supporting Information).

### The PM-ER Axis

One of the intriguing findings from this analysis was the apparent cosegregation of ER with the PM. This ER protein population at the PM (Supplemental Table S7, Supporting Information) constitutes approximately 14% of all annotated mouse ER proteins raising the possibility that this may represent a unique subset of ER proteins. However, a comparison between the PM-associated ER protein population and the total mouse ER protein population by GO analysis revealed no evidence for the selective enrichment of a particular subpopulation of the ER (Supplemental Table S7, Supporting Information). To verify the

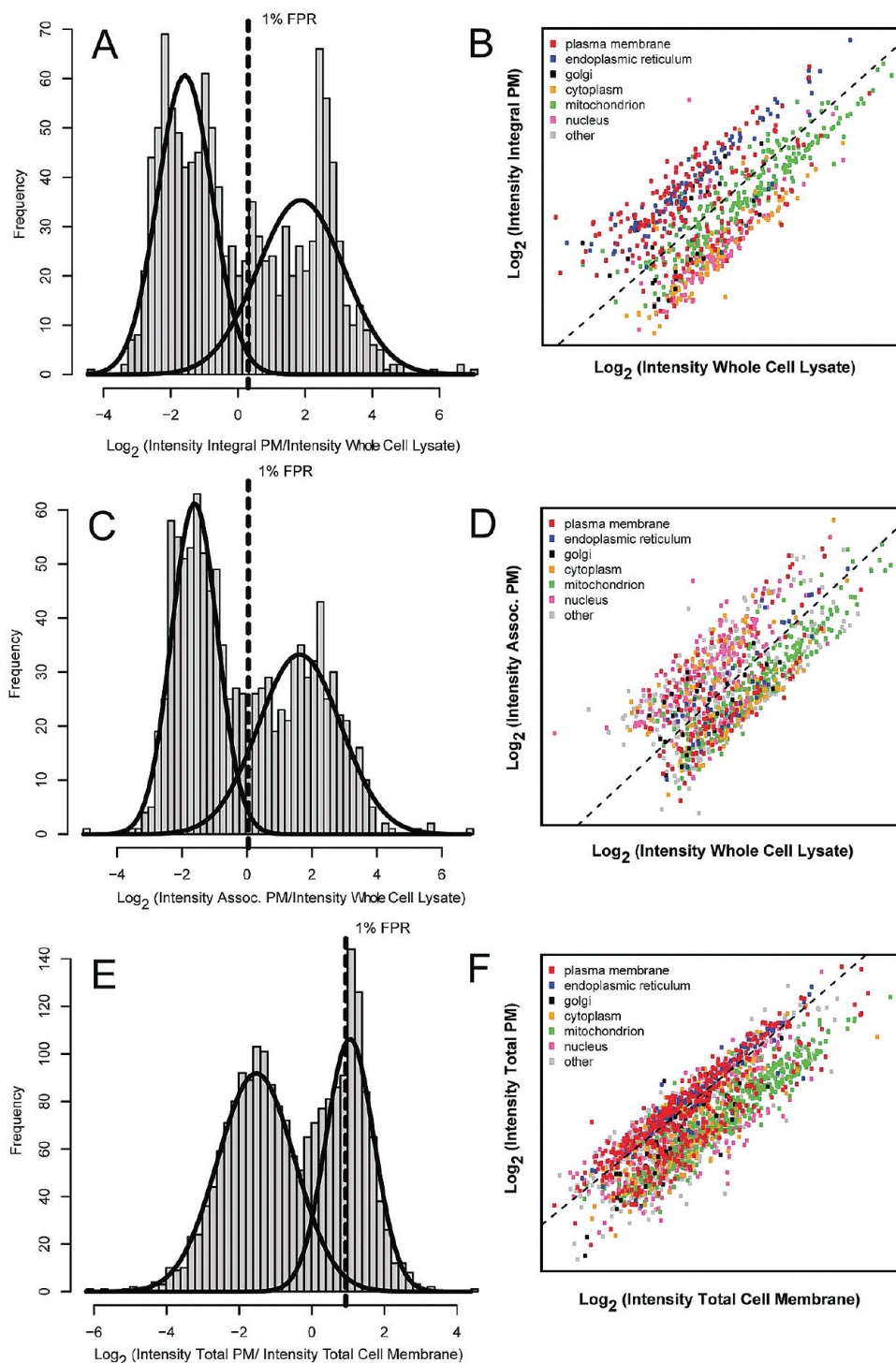


**Figure 3.** Relative enrichment analysis of the cationic silica PM fraction from whole cell lysate and total cell membrane. Double SILAC labeled 3T3-L1 fibroblasts were differentiated into adipocytes and serum-starved for 2–3 h. Cationic silica PM fractions were mixed with whole cell lysate or total cell membrane and the proteins analyzed by LC–MS/MS (Figure 2). Raw mass spectrometry data was analyzed by the MaxQuant software program and all ratios were calculated from the raw intensities. (A) Integral cationic silica PM/whole cell lysate ratios were converted to a binary logarithm and plotted against frequency prior to mixture modeling. (B) Raw intensities for each protein from both the integral cationic silica PM fraction and the whole cell lysate were converted to a binary logarithm and plotted against each other. Proteins were classified by subcellular location as described in the “Materials and Methods”. The same analysis was performed for the associated cationic silica PM fraction combined with the whole cell lysate (B and C) and the total cationic silica PM fraction (integral and associated) combined with total cell membrane (E and F). In each case, the dotted line represents a false positive rate (FPR) of 1% and proteins to the right of this line (A, C, E) or above it (B, D, F) were classified as PM. See also Supplemental Tables S2, S3 and S4 (Supporting Information).

association between the ER and the PM in adipocytes, we expressed an ER-directed HRP fusion protein (KDEL-HRP) in

adipocytes and used this to visualize the ER by electron microscopy (EM). Consistent with our prediction, ER elements close

**Table 1. Protein Functional Groups Enriched in the Adipocyte PM Proteome<sup>a</sup>**

	adipocyte PM	% ontology term
<b>G-proteins</b>	41	15
G-protein modulator	22	6
Large G-protein	14	27
<b>Transporters</b>	38	6
Cation	14	8
ATP-binding cassette	4	9
Amino acid	2	6
Carbohydrate	2	6
<b>Receptors</b>	32	1
Tyrosine protein kinase	7	9
Immunoglobulin	2	2
<b>Ion Channels</b>	8	2
Voltage-gated	2	2
<b>Others</b>		
Regulatory molecules	69	6
Cytoskeletal protein	47	6
Membrane traffic proteins	36	11
Hydrolases	28	4
Small GTPase	26	13
Cell adhesion molecules	23	6
Kinases	23	3
SNAREs	8	21

<sup>a</sup> All unique proteins enriched from the whole cell lysate and total cell membrane preparations were manually curated as described in Materials and Methods, and the resulting list of proteins was subjected to gene set enrichment analysis by Panther molecular function (Table S5, Supporting Information). A select number of functional groups are represented and the number of proteins identified for each is shown on the left. On the right this value is expressed as a percentage of all annotated proteins in that functional group.

to the PM were very common in adipocytes, with numerous putative ER-PM contacts, in which the ER was closely apposed to the PM, evident by EM (Figure 4). These data likely explain the observed cofractionation of ER with the PM and, more importantly, are suggestive of a unique functional association between these two organelles in the adipocyte.

### Survey of Insulin Action at the PM

One of the notable features of the adipocyte PM is its ability to modulate its polypeptide composition under certain conditions. For example, insulin stimulation rapidly increases the amount of the glucose transporter GLUT4 found at the PM and this process plays an important role in the postprandial disposal of glucose. To further explore the adaptability of the adipocyte PM in response to insulin stimulation we designed a SILAC based experiment, using cationic silica, to identify insulin responsive PM proteins from our adipocyte PM proteome (Figure 5A). Adipocytes were stimulated with 100 nM insulin for 20 min to induce maximal levels of cell surface GLUT4<sup>30</sup> maximizing the possibility for identification of novel insulin responsive PM proteins. The phosphatidylinositol-3-kinase (PI3K) inhibitor, wortmannin was utilized in the presence of insulin to identify insulin responsive proteins downstream of PI3K.

Using a high stringency filter ( $p < 0.05$ , Significance level B) for insulin responsive proteins detected in at least two independent experiments, we identified 30 proteins (Supplemental Tables

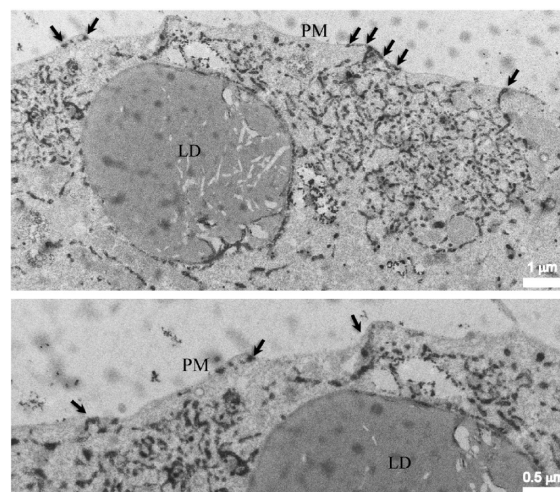


**Figure 4.** Ultrastructural characterization of the ER in differentiated 3T3-L1 adipocytes using an ER-directed HRP fusion protein (KDEL-HRP). The arrows mark regions of the ER labeled with the electron dense HRP reaction product which are very closely apposed to the PM. LD, lipid droplet.

S8 and S9, Supporting Information). Among these, 8 were present in the PM proteome. All 8 proteins underwent an insulin-dependent increase in PM association in a PI3K-dependent manner and included GLUT4, IRAP and the transferrin receptor (TfR), all of which have previously been described as insulin responsive proteins in the adipocyte<sup>8,31</sup> (Figure 5B). Among the novel insulin-responsive proteins were four collagen isoforms, (Col3a1 and Col6a1, 2 and 3) as well as the sodium/hydrogen exchanger, NHE6 (SLC9A6) (Figure 5B).

### The Sodium/Hydrogen Exchanger, NHE6 is a Novel Insulin-Responsive Protein

The insulin-dependent translocation of Collagen alpha-1(VI) chain (Col6a1) and NHE6 to the PM was verified by immunoblotting using specific antibodies to each (Figure 6A). The Col6a1 antibody labeled a band of the expected size at approximately 120 kDa. The NHE6 antibody labeled multiple bands between 64 and 250 kDa, consistent with previous studies that observed a mature, glycosylated form at 90–100 kDa and an immature, less glycosylated form at approximately 64 kDa.<sup>32</sup> The more mature form of NHE6 at 98 kDa appeared to be the insulin-responsive form and thus was the focus of the remaining studies (Figure 6A). It has also been suggested that NHE6 is subject to aggregation as is the case for many polytopic membrane proteins<sup>32</sup> and that this may account for the larger band observed at 250 kDa. NHE6 was selected for more detailed analysis and an investigation of the expression of this transporter in a range of tissues indicated that it is expressed at high levels in the brain as well as in a number of insulin responsive tissues including the liver, kidney and adipose tissue (Figure 6B). To further investigate the role of NHE6 in adipose tissue, we analyzed NHE6 protein levels during the adipocyte differentiation time course (Figure 6C). NHE6 was expressed at low levels in preadipocytes and its expression was markedly upregulated during adipocyte differentiation with a similar time course to that observed for GLUT4 (not shown). Insulin stimulates GLUT4 translocation to the PM via increased exocytosis of GLUT4 storage vesicles (GSV).<sup>3</sup> To determine if NHE6 is similarly regulated we first investigated the subcellular distribution of NHE6 in 3T3-L1 adipocytes in the

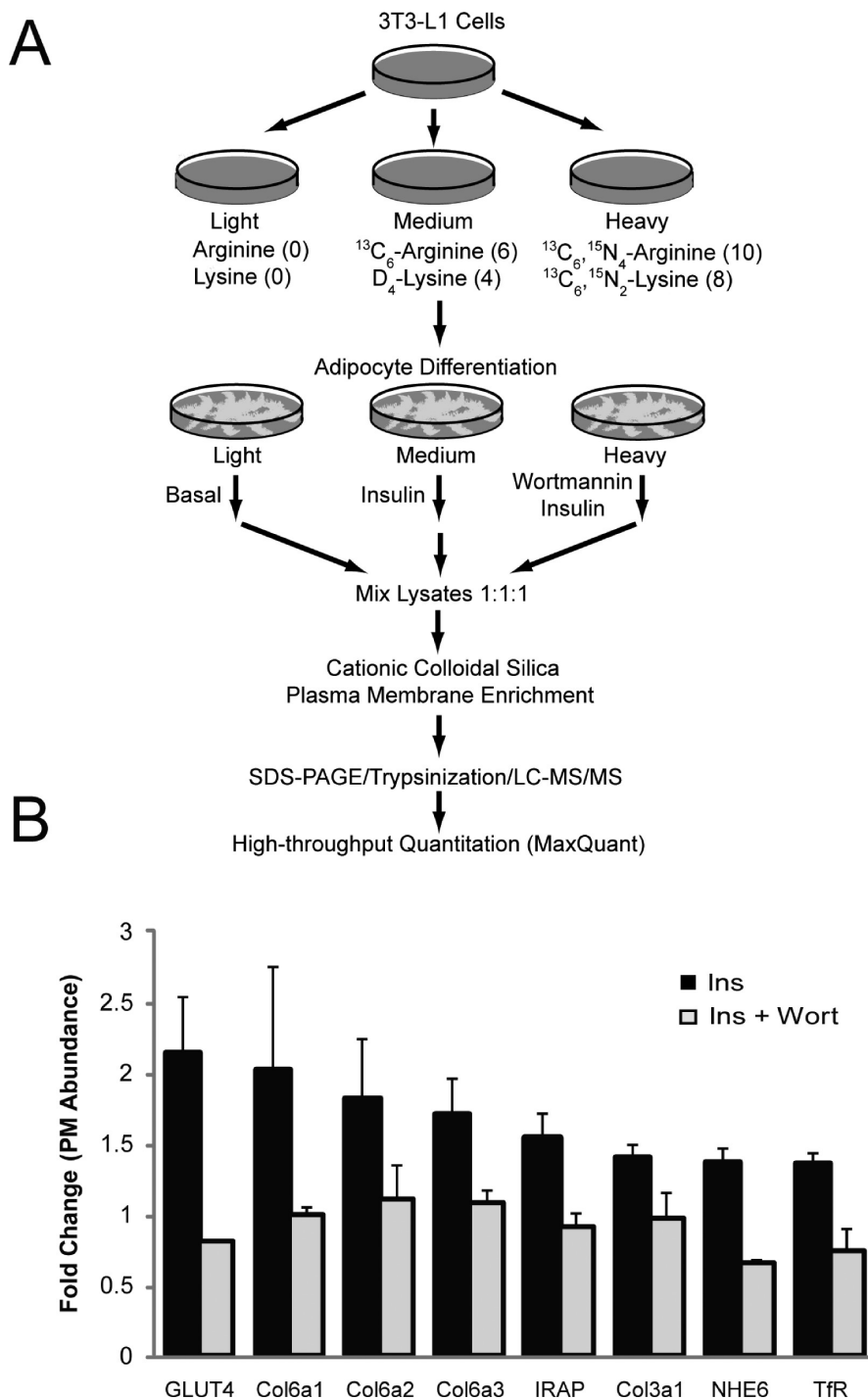


**Figure 5.** Insulin-responsive proteins at the adipocyte PM (A) 3T3-L1 fibroblasts were triple SILAC labeled as shown and differentiated into adipocytes. Adipocytes were serum-starved for 3 h and then either left untreated (Basal) (light label), treated with insulin (100 nM, 20 min) (medium label) or treated with wortmannin and insulin (100 nM wortmannin, 20 min prior to insulin stimulation) (heavy label). Following treatment, adipocyte membranes were coated with silica, the cells lysed and mixed and the PM isolated and further fractionated using cationic colloidal silica combined with a high salt, high pH wash. The isolated proteins were then separated by SDS-PAGE and the entire gel lane digested with trypsin and analyzed by LC-MS/MS. The raw mass spectrometry data was analyzed by the MaxQuant software program. (B) Relative abundance of insulin-responsive PM proteins identified by SILAC analysis. SILAC labeled 3T3-L1 adipocytes were incubated with (medium) or without insulin (100 nM) for 20 min (light) in the absence or presence of wortmannin (100 nM) (heavy) and peptides were analyzed as described above. Data represent mean  $\pm$  SD of medium/light and heavy/light ratios from three independent experiments. See also Supplemental Tables S8 and S9 (Supporting Information).

presence and absence of insulin. NHE6 displayed a similar subcellular distribution to GLUT4 and another GSV component, IRAP and it underwent insulin-dependent movement from the

low density microsomal (LDM) fraction to the PM with insulin (Figure 6D). This suggests that NHE6 may translocate together with GLUT4 and IRAP and thus reside in the same compartment.

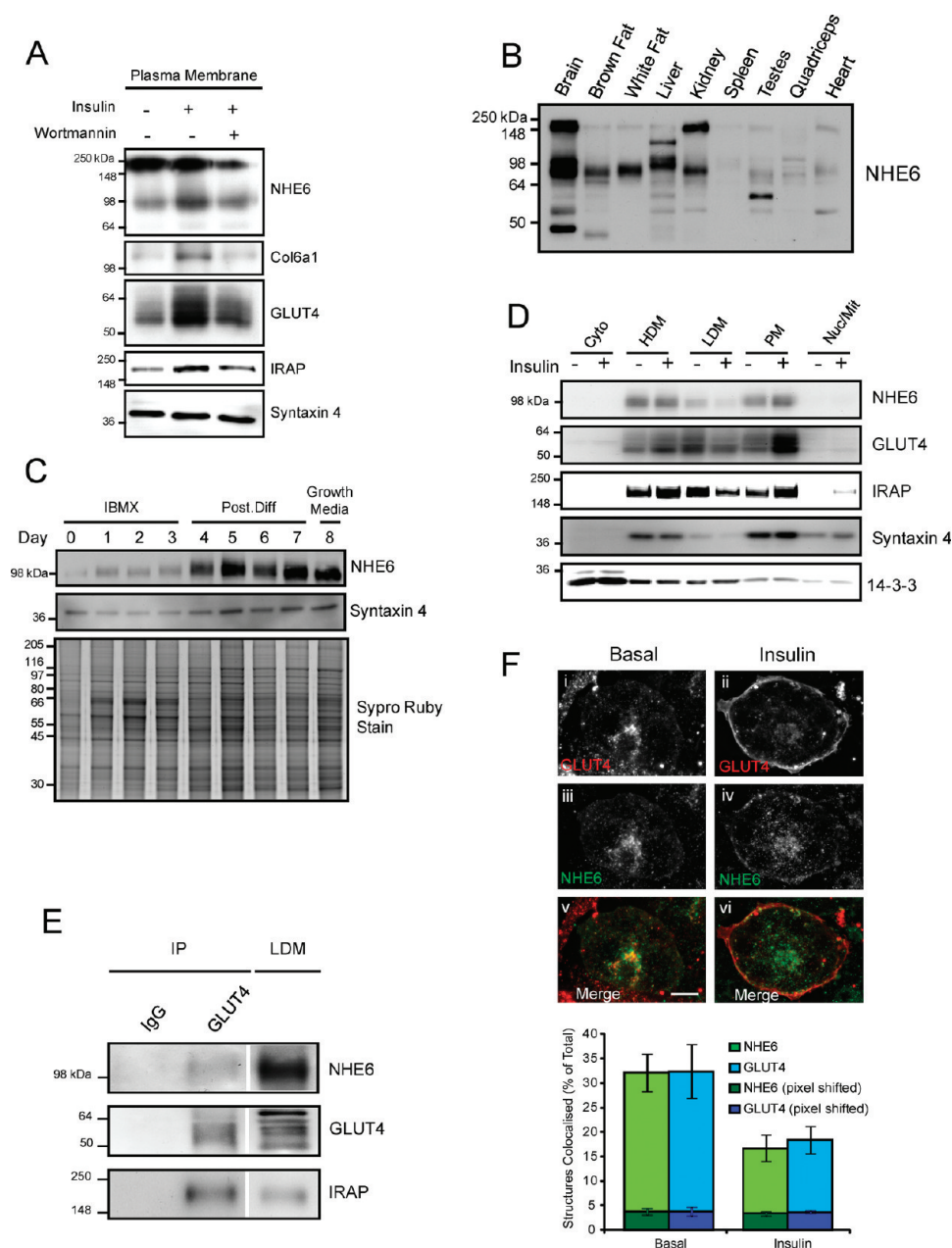


**Figure 6.** NHE6 is a novel insulin-responsive PM protein. (A) NHE6 and Col6a1 translocate to the PM in the presence of insulin. Cationic colloidal silica integral PM fractions were obtained from serum starved 3T3-L1 adipocytes (3 h) which were either left untreated (basal), treated with insulin (100 nM, 20 min) or treated with wortmannin and insulin (100 nM wortmannin, 20 min prior to insulin) and analyzed by Western blot with the use of anti-NHE6, anti-Col6a1, anti-GLUT4, anti-IRAP and anti-Syntaxin 4 antibodies. The experiment was performed three times and images are from a representative experiment. (B) Tissue distribution of NHE6 protein expression. Mouse tissues were collected and the lysates analyzed by Western blot with the use of anti-NHE6 antibody. The experiment was performed twice and the images are from a representative experiment. (C) NHE6 protein expression during 3T3-L1 adipocyte differentiation. Lysates from differentiating 3T3-L1 fibroblasts were collected on the days indicated and analyzed by Western blot with the use of anti-NHE6 and anti-Syntaxin 4 antibodies. A SYPRO ruby protein stain of the membrane was included as a loading control. The experiment was performed twice and the images are from a representative experiment. (D) Subcellular distribution of NHE6 protein expression in the presence of insulin. Basal (3 h) and insulin treated (100 nM, 20 min) 3T3-L1 adipocytes were fractionated into cytosol, high density microsomes (HDM), low density microsomes (LDM), plasma membrane (PM) and mitochondria/nucleus. Equal amounts of protein for each fraction were analyzed by Western blot with the use of anti-NHE6, anti-GLUT4, anti-IRAP, anti-Syntaxin 4 and anti-14-3-3 antibodies. The experiment was performed twice and the images are from a representative experiment. (E) NHE6 associates with GLUT4 storage vesicles. The low density microsome fraction (LDM) was obtained from 3 h serum-starved 3T3-L1 adipocytes and subjected to immunoprecipitation (IP) with anti-GLUT4 and irrelevant antibodies (IgG). Immunoprecipitates and LDM fractions were analyzed by Western blot with the use of anti-NHE6, anti-GLUT4 and anti-IRAP antibodies. The experiment was performed two times and the images are from a representative experiment. (F) Immunofluorescence analysis of NHE6 and GLUT4 colocalization. Serum-starved (basal, 3 h) and insulin-stimulated (100 nM, 20 min) 3T3-L1 adipocytes were fixed, permeabilized and stained with anti-GLUT4 and anti-NHE6 antibodies. GLUT4 and NHE6 were detected using Cy3- (red) and Cy2- (green) conjugated secondary antibodies, respectively and the amount of internal structure colocalization quantitated by IMARIS\_64 v6.2.1 (Bitplane) software. Images were pixel shifted by the equivalent of 200 nm and reanalyzed to validate the data. Data represent mean  $\pm$  SEM of values from 3–4 cells from two independent experiments. Bar, 15  $\mu$ m.

To test this, we immuno-isolated GSVs using a GLUT4-specific antibody and found that both NHE6 and IRAP were enriched in these vesicles (Figure 6E). Furthermore, we observed significant colocalization between GLUT4 and NHE6 in adipocytes using confocal immunofluorescence microscopy (Figure 6F). Following insulin stimulation, there was a marked translocation of both NHE6 and GLUT4 to the PM (Figure 6F, panels ii and iv) and a reduction in the intracellular colocalization between both proteins, indicating that around half of the colocalized NHE6 protein is present in insulin-responsive GSVs.

## DISCUSSION

In this study we have used subcellular fractionation combined with SILAC enrichment, LC-MS/MS and statistical analysis to dissect the polypeptide composition of the adipocyte PM. Similar approaches have been developed for characterization of other cellular organelles<sup>26–28</sup> and here we have adapted these to identify highly enriched proteins from a mixture of PM and whole cell lysate or total cell membrane and eliminate, by an unbiased means, a large number of contaminating proteins from an already relatively pure cationic silica PM fraction. The power of this analysis is demonstrated by the fact that the cationic silica PM fraction is highly enriched in GO annotated PM proteins relative to the whole cell lysate or total cell membrane fraction but is not enriched in mitochondrial proteins despite the large number of these proteins present. These analyses, combined with the use of poly(acrylic acid) partial sodium salt solution to minimize nonspecific protein:silica interactions<sup>11</sup> and manual curation, allowed us to produce a high confidence list of 486 *bona fide* adipocyte PM proteins. This compendium comprises a relatively restricted representation of certain protein families such as receptor tyrosine kinases as well as 30 proteins with no known subcellular location, providing scope for new insights into the unique function of the adipocyte. Moreover, this analysis led us to identify an enrichment of ER-PM contact sites in the adipocyte that could well play a unique role in lipid metabolism in this cell. Our studies of the adipocyte PM in the presence of insulin have provided greater insight into the actions of this hormone leading to the identification of the sodium/hydrogen exchanger, NHE6 as well as several other novel insulin-regulated proteins.

The compendium contains many of the components expected of a generic PM including cytoskeleton, extracellular matrix, vesicle transport proteins, proteins regulating endocytosis and nutrient regulatory molecules such as transporters and channels. There are several features of the resource that are noteworthy. First, the fat cell expresses a limited repertoire of receptor proteins and indeed this is considered to be a major factor that determines cellular specificity. In regard to receptor tyrosine kinases (RTKs), the insulin receptor was the major member of this family found at the fat cell PM. We also detected lower levels of the PDGFR consistent with previous studies<sup>33</sup> but no other members of the RTK growth factor family were detected. Hence, this likely provides key insight into the ability of the fat cell to maintain inordinate specificity with respect to insulin regulation of glucose metabolism because it would appear that there are few other receptors on the surface of these cells capable of activating the PI3K/Akt pathway. We did not detect the IGF-1 receptor despite the fact that this protein has previously been observed in adipocytes.<sup>34,35</sup> This suggests that our compendium is not a definitive list and that we are probably missing some of the low abundance proteins. In terms of G-protein coupled receptors

(GPCRs), which are high priority drug targets with numerous family members, we only detected one of these proteins, GPRC5B, an orphan receptor with no known function. However, a large number of heterotrimeric G-proteins and G-protein modulators known to act downstream of GPCRs were identified among our PM compendium including Phospholipase C-beta-3, several guanine nucleotide-binding subunits and adenylate cyclase-stimulating G alpha, suggesting that there are perhaps other, low abundant GPCRs on the adipocyte PM, such as beta-adrenergic receptors, that were not detected in this study.

Second, in as far as the trafficking of GLUT4 to the membrane, in addition to known molecules such as Munc18c, Syntaxin4, SNAP23, 6 subunits of the exocyst complex, Myosin 1c, Rab14, Rab10, Rab8, VAMP2 and VAMP3 and extended synaptotagmin 1 (E-Syt1),<sup>36</sup> we also identified a range of others including dysferlin, the RabGAP TBC1D24, Rab21, Rab34, Rab35, Myosin-9, Sorting nexin9, 14, and 18 as well as a second member of the synaptotagmin family, E-Syt2. Third, approximately 20% of the adipocyte PM proteome was comprised of proteins with no known cellular compartment. The identification of these proteins as components of the fat cell PM provides important additional information about these molecules. Many of these are transmembrane proteins and so they represent potential new adipocyte specific targets worthy of future study. Progesterone and adipoQ receptor 4 (PAQR4) is an example of such a protein. The PAQR proteins which include the adiponectin receptors, AdipoR1 (PAQR1) and AdipoR2 (PAQR2) are highly homologous to alkaline ceramidase and upon activation are associated with increased ceramidase activity, reduced intracellular ceramide levels and improved insulin sensitivity.<sup>37,38</sup> It will be interesting to determine whether PAQR4 also regulates ceramide levels and insulin sensitivity in the adipocyte.

Other proteins identified at the adipocyte PM with potential roles in the regulation of insulin sensitivity include Heme oxygenase (HO)-1 and -2, Paraoxanase 2, Cathepsin L and Cystatin C. HO preserves cell viability and function during increasing levels of oxidative stress and hypoxia<sup>39</sup> and regulates insulin sensitivity in rodents.<sup>40</sup> Paraoxanase 2 is another cellular antioxidant that also exerts a positive influence on insulin sensitivity.<sup>41</sup> In contrast, Cathepsin L-deficient mice are lean and more insulin sensitive than wild type littermates.<sup>42</sup> Cathepsin L is a secreted, cysteine protease involved in the regulation of ECM remodelling while Cystatin C is an endogenous inhibitor of this protease family, which is also associated with obesity.<sup>43</sup> We identified a number of other extracellular hydrolases at the adipocyte PM, including MMP14, ATP13A and ABHD1,6 and 15. Similar to Cathepsin L, MMP14 has been linked to the regulation of adipogenesis,<sup>44</sup> while ATP13A and ABHD1,6 and 15 currently have no known function. Given the critical role played by the ECM in adipocyte differentiation and function, it will be important to identify and characterize these and other potential ECM proteases in future studies.

We also utilized this methodology to interrogate changes in the PM proteome in response to insulin. In addition to the identification of a number of well described insulin-regulated proteins including GLUT4 and IRAP, we also identified the sodium/hydrogen exchanger, NHE6 as well as four insulin responsive collagens, three of which (Col6A1–3) are known to form a complex. Mutations in these three genes lead to unusual forms of muscular dystrophy and recent studies indicate that Collagen VI plays an important role in the regulation of insulin sensitivity and Akt signaling.<sup>45</sup> NHE6 functions as an antiporter

to leak  $H^+$  from the lumen of vesicles/organelles into the cytosol in exchange for  $Na^+$  and therefore plays an important role in maintaining intracellular pH.<sup>46</sup> Like other proteins that translocate to the PM upon insulin stimulation such as low density lipoprotein receptor-related protein 1 (LRP1), IRAP and GLUT4,<sup>8,31</sup> NHE6 is also found in GSVs. LRP1 was not detected in the present study possibly because it is a large protein (~500 kDa) and it may not have entered the 10% acrylamide gel used during SDS-PAGE analysis.<sup>31</sup> Nevertheless, these findings suggest that the exocytosis of GSVs modulate a number of cellular actions including glucose and lipid metabolism as well as pH. It is well established that insulin and other growth factors induce cytosolic alkalization and this is thought to play an essential role in the cellular effects of hormones like insulin.<sup>47,48</sup> A picture is now emerging that this regulation is quite complex. It has been reported that insulin stimulates phosphorylation of both NHE1 and NHE3 and that this results in an increase in their catalytic activity.<sup>49,50</sup> In addition, it has recently been shown that insulin induces the PM translocation of NHE1 in cardiomyocytes;<sup>51</sup> although we did not observe this in the adipocyte. Therefore, the observation that insulin also stimulates the translocation of NHE6 to the PM in adipocytes adds to this growing list of pH regulators. It would be of interest to determine whether both NHE1 and NHE6 can translocate to the PM in primary adipocytes and other insulin responsive tissues upon insulin stimulation.

Notably, few PM proteins, including alpha-actin-1 and keratin-76 exhibited a significant decrease in PM association following insulin stimulation. Interestingly both of these proteins are associated with the cytoskeleton and are reduced in PM abundance in a PI3K-independent manner. Given the important role of the cytoskeleton in the regulation of many insulin-dependent processes such as GLUT4 trafficking and cell migration, this finding warrants further investigation.

Contacts between the ER and PM were first described in yeast as PM associated membrane (PAM) and have since been reported in several cell types.<sup>52–54</sup> PAM has a high phosphatidylserine, phosphatidylinositol and cholesterol synthesizing capacity and is associated with the regulation of capacitive calcium influx.<sup>52,54</sup> The proliferation of cortical ER attached to the PM in the adipocyte may have important implications, in view of the key role of the ER in lipid biosynthesis. Such an arrangement would be particularly beneficial to a cell such as the adipocyte which must constantly handle a large volume of lipid traffic. Notably, there were a number of PAM-associated proteins enriched at the adipocyte PM, including squalene synthase and epoxidase, STIM1 and 2, PTP1B,  $Na^+/K^+$ -ATPase and SERCA.<sup>53–55</sup> The lipid transfer proteins NIR2, SCP2 and OSBP as well as the OSBP-interacting partners VAP and ARF1 which are associated with the non vesicular trafficking of sterol and phospholipids between the ER and PM were also enriched at the PM.<sup>53</sup> This provides additional evidence of an association between these organelles in the adipocyte. Although previous studies have not reported an enrichment of ER together with the PM, this is likely a reflection of the methodology used for fractionation of the cells which may not have preserved these ER-PM contacts.

Together, these findings of the adipocyte PM have provided greater insight into the proteomic architecture of this organelle and its interactions with the intra- and extracellular environments. We have uncovered an association between the PM and the ER in the adipocyte and have identified many novel PM proteins, some with no known function and others with potential roles in the regulation of insulin sensitivity and adipogenesis.

This work has provided a snapshot of druggable molecules like GPCRs, RTKs and channels that are found at the adipocyte PM and is a rich resource for future studies on the adipocyte.

## ■ ASSOCIATED CONTENT

### Supporting Information

Supplemental figures and full analysis of LC–MS/MS data as Supplemental tables. This material is available free of charge via the Internet at <http://pubs.acs.org>.

## ■ AUTHOR INFORMATION

### Corresponding Author

\*Tel. +61292958210; Fax. +61292958201, E-mail: [d.james@garvan.org.au](mailto:d.james@garvan.org.au).

### Author Contributions

<sup>†</sup>These authors contributed equally to this work.

### Notes

<sup>‡</sup>Deceased, October, 2009.

## ■ ACKNOWLEDGMENT

We thank D. Beer Stolz (University of Pittsburgh) for providing the cationic silica and A. Cooper, C. Schmitz-Peiffer, D. Fazakerley and G. Cooney for critical review of the manuscript. The Bioanalytical Mass Spectrometry Facility, UNSW, was supported in part by grants from the Australian Government Systemic Infrastructure Initiative and Major National Research Facilities Program (UNSW node of the Australian Proteome Analysis Facility) and by the UNSW Capital Grants Scheme. This work was supported by grants from the NHMRC of Australia and Diabetes Australia Research Trust (to D.E.J.). The authors wish to express their condolences to the friends and family of Michael Guilhaus who sadly passed away in October, 2009.

## ■ REFERENCES

- (1) Guilherme, A.; Virbasius, J. V.; Puri, V.; Czech, M. P. Adipocyte dysfunction linking obesity to insulin resistance and type 2 diabetes. *Nat. Rev. Mol. Cell Biol.* **2008**, *9* (5), 367–77.
- (2) Rowland, A. F.; Fazakerley, D. J.; James, D. E. Mapping insulin/GLUT4 circuitry. *Traffic* **2011**, *12* (6), 672–81.
- (3) Bryant, N. J.; Govers, R.; James, D. E. Regulated transport of the glucose transporter GLUT4. *Nat. Rev. Mol. Cell Biol.* **2002**, *3* (4), 267–77.
- (4) Ryder, J. W.; Yang, J.; Galuska, D.; Rincon, J.; Bjornholm, M.; Krook, A.; Lund, S.; Pedersen, O.; Wallberg-Henriksson, H.; Zierath, J. R.; Holman, G. D. Use of a novel impermeable biotinylated photolabeling reagent to assess insulin- and hypoxia-stimulated cell surface GLUT4 content in skeletal muscle from type 2 diabetic patients. *Diabetes* **2000**, *49* (4), 647–54.
- (5) Zierath, J. R.; He, L.; Guma, A.; Odegaard Wahlstrom, E.; Klip, A.; Wallberg-Henriksson, H. Insulin action on glucose transport and plasma membrane GLUT4 content in skeletal muscle from patients with NIDDM. *Diabetologia* **1996**, *39* (10), 1180–9.
- (6) Ong, S. E.; Blagoev, B.; Kratchmarova, I.; Kristensen, D. B.; Steen, H.; Pandey, A.; Mann, M. Stable isotope labeling by amino acids in cell culture, SILAC, as a simple and accurate approach to expression proteomics. *Mol. Cell. Proteomics* **2002**, *1* (5), 376–86.
- (7) Connolly, C. N.; Futter, C. E.; Gibson, A.; Hopkins, C. R.; Cutler, D. F. Transport into and out of the Golgi complex studied by

transfecting cells with cDNAs encoding horseradish peroxidase. *J. Cell Biol.* **1994**, *127* (3), 641–52.

(8) Larance, M.; Ramm, G.; Stockli, J.; van Dam, E. M.; Winata, S.; Wasinger, V.; Simpson, F.; Graham, M.; Junutula, J. R.; Guilhaus, M.; James, D. E. Characterization of the role of the Rab GTPase-activating protein AS160 in insulin-regulated GLUT4 trafficking. *J. Biol. Chem.* **2005**, *280* (45), 37803–13.

(9) Shewan, A. M.; van Dam, E. M.; Martin, S.; Luen, T. B.; Hong, W.; Bryant, N. J.; James, D. E. GLUT4 recycles via a trans-Golgi network (TGN) subdomain enriched in Syntaxins 6 and 16 but not TGN38: involvement of an acidic targeting motif. *Mol. Biol. Cell* **2003**, *14* (3), 973–86.

(10) Olsen, J. V.; Blagoev, B.; Gnadt, F.; Macek, B.; Kumar, C.; Mortensen, P.; Mann, M. Global, in vivo, and site-specific phosphorylation dynamics in signaling networks. *Cell* **2006**, *127* (3), 635–48.

(11) Chaney, L. K.; Jacobson, B. S. Coating cells with colloidal silica for high yield isolation of plasma membrane sheets and identification of transmembrane proteins. *J. Biol. Chem.* **1983**, *258* (16), 10062–72.

(12) Zhao, Y.; Zhang, W.; Kho, Y. Proteomic analysis of integral plasma membrane proteins. *Anal. Chem.* **2004**, *76* (7), 1817–23.

(13) Hoehn, K. L.; Hohnen-Behrens, C.; Cederberg, A.; Wu, L. E.; Turner, N.; Yuasa, T.; Ebina, Y.; James, D. E. IRS1-independent defects define major nodes of insulin resistance. *Cell Metab.* **2008**, *7* (5), 421–33.

(14) Larance, M.; Rowland, A. F.; Hoehn, K. L.; Humphreys, D. T.; Preiss, T.; Guilhaus, M.; James, D. E. Global phosphoproteomics identifies a major role for AKT and 14–3-3 in regulating EDC3. *Mol. Cell. Proteomics* **2010**, *9* (4), 682–94.

(15) Haas, W.; Faherty, B. K.; Gerber, S. A.; Elias, J. E.; Beausoleil, S. A.; Bakalarski, C. E.; Li, X.; Villen, J.; Gygi, S. P. Optimization and use of peptide mass measurement accuracy in shotgun proteomics. *Mol. Cell. Proteomics* **2006**, *5* (7), 1326–37.

(16) Cox, J.; Mann, M. MaxQuant enables high peptide identification rates, individualized p.p.b.-range mass accuracies and proteome-wide protein quantification. *Nat. Biotechnol.* **2008**, *26* (12), 1367–72.

(17) Stockli, J.; Davey, J. R.; Hohnen-Behrens, C.; Xu, A.; James, D. E.; Ramm, G. Regulation of glucose transporter 4 translocation by the Rab guanine nucleotide exchange factor AS160/TBC1D4: role of phosphorylation and membrane association. *Mol. Endocrinol.* **2008**, *22* (12), 2703–15.

(18) Dennis, G., Jr.; Sherman, B. T.; Hosack, D. A.; Yang, J.; Gao, W.; Lane, H. C.; Lempicki, R. A. DAVID: Database for Annotation, Visualization, and Integrated Discovery. *Genome Biol.* **2003**, *4* (5), P3.

(19) Krogh, A.; Larsson, B.; von Heijne, G.; Sonnhammer, E. L. Predicting transmembrane protein topology with a hidden Markov model: application to complete genomes. *J. Mol. Biol.* **2001**, *305* (3), 567–80.

(20) da Cunha, J. P.; Galante, P. A.; de Souza, J. E.; de Souza, R. F.; Carvalho, P. M.; Ohara, D. T.; Moura, R. P.; Oba-Shinja, S. M.; Marie, S. K.; Silva, W. A., Jr.; Perez, R. O.; Stransky, B.; Pieprzyk, M.; Moore, J.; Caballero, O.; Gama-Rodrigues, J.; Habr-Gama, A.; Kuo, W. P.; Simpson, A. J.; Camargo, A. A.; Old, L. J.; de Souza, S. J. Bioinformatics construction of the human cell surfaceome. *Proc. Natl. Acad. Sci. U.S.A.* **2009**, *106* (39), 16752–7.

(21) Zdobnov, E. M.; Apweiler, R. InterProScan—an integration platform for the signature-recognition methods in InterPro. *Bioinformatics* **2001**, *17* (9), 847–8.

(22) R Development Core Team. *R: A language and Environment for Statistical Computing*; R Foundation for Statistical Computing: Vienna, 2009.

(23) Fraley, C.; Raftery, A. E. *MCLUST Version 3 for R: Normal Mixture Modeling and Model-based Clustering*; Department of Statistics, University of Washington: Seattle, WA, 2006; p 504.

(24) Adachi, J.; Kumar, C.; Zhang, Y.; Mann, M. In-depth analysis of the adipocyte proteome by mass spectrometry and bioinformatics. *Mol. Cell. Proteomics* **2007**, *6* (7), 1257–73.

(25) Ashburner, M.; Ball, C. A.; Blake, J. A.; Botstein, D.; Butler, H.; Cherry, J. M.; Davis, A. P.; Dolinski, K.; Dwight, S. S.; Eppig, J. T.; Harris, M. A.; Hill, D. P.; Issel-Tarver, L.; Kasarskis, A.; Lewis, S.; Matese, J. C.;

Richardson, J. E.; Ringwald, M.; Rubin, G. M.; Sherlock, G. Gene ontology: tool for the unification of biology. The Gene Ontology Consortium. *Nat. Genet.* **2000**, *25* (1), 25–9.

(26) Andersen, J. S.; Wilkinson, C. J.; Mayor, T.; Mortensen, P.; Nigg, E. A.; Mann, M. Proteomic characterization of the human centrosome by protein correlation profiling. *Nature* **2003**, *426* (6966), 570–4.

(27) Forner, F.; Kumar, C.; Lubner, C. A.; Fromme, T.; Klingenspor, M.; Mann, M. Proteomic differences between brown and white fat mitochondria reveal specialized metabolic functions. *Cell Metab.* **2009**, *10* (4), 324–35.

(28) Marelli, M.; Nesvizhskii, A. I.; Aitchison, J. D. Identifying bona fide components of an organelle by isotope-coded labeling of subcellular fractions: an example in peroxisomes. *Methods Mol. Biol.* **2008**, *432*, 357–71.

(29) Andreyev, A. Y.; Shen, Z.; Guan, Z.; Ryan, A.; Fahy, E.; Subramaniam, S.; Raetz, C. R.; Briggs, S.; Dennis, E. A. Application of proteomic marker ensembles to subcellular organelle identification. *Mol. Cell. Proteomics* **2010**, *9* (2), 388–402.

(30) Govers, R.; Coster, A. C.; James, D. E. Insulin increases cell surface GLUT4 levels by dose dependently discharging GLUT4 into a cell surface recycling pathway. *Mol. Cell. Biol.* **2004**, *24* (14), 6456–66.

(31) Jedrychowski, M. P.; Gartner, C. A.; Gygi, S. P.; Zhou, L.; Herz, J.; Kandror, K. V.; Pilch, P. F. Proteomic analysis of GLUT4 storage vesicles reveals LRP1 to be an important vesicle component and target of insulin signaling. *J. Biol. Chem.* **2010**, *285* (1), 104–14.

(32) Ohgaki, R.; Fukura, N.; Matsushita, M.; Mitsui, K.; Kanazawa, H. Cell surface levels of organellar Na<sup>+</sup>/H<sup>+</sup> exchanger isoform 6 are regulated by interaction with RACK1. *J. Biol. Chem.* **2008**, *283* (7), 4417–29.

(33) Vaziri, C.; Faller, D. V. Down-regulation of platelet-derived growth factor receptor expression during terminal differentiation of 3T3-L1 pre-adipocyte fibroblasts. *J. Biol. Chem.* **1996**, *271* (23), 13642–8.

(34) Rubin, C. S.; Hirsch, A.; Fung, C.; Rosen, O. M. Development of hormone receptors and hormonal responsiveness in vitro. Insulin receptors and insulin sensitivity in the preadipocyte and adipocyte forms of 3T3-L1 cells. *J. Biol. Chem.* **1978**, *253* (20), 7570–8.

(35) Smith, P. J.; Wise, L. S.; Berkowitz, R.; Wan, C.; Rubin, C. S. Insulin-like growth factor-I is an essential regulator of the differentiation of 3T3-L1 adipocytes. *J. Biol. Chem.* **1988**, *263* (19), 9402–8.

(36) Lalioti, V.; Muruais, G.; Dinarina, A.; van Damme, J.; Vandekerckhove, J.; Sandoval, I. V. The atypical kinase Cdk5 is activated by insulin, regulates the association between GLUT4 and E-Syt1, and modulates glucose transport in 3T3-L1 adipocytes. *Proc. Natl. Acad. Sci. U.S.A.* **2009**, *106* (11), 4249–53.

(37) Holland, W. L.; Miller, R. A.; Wang, Z. V.; Sun, K.; Barth, B. M.; Bui, H. H.; Davis, K. E.; Bikman, B. T.; Halberg, N.; Rutkowski, J. M.; Wade, M. R.; Tenorio, V. M.; Kuo, M. S.; Brozinick, J. T.; Zhang, B. B.; Birnbaum, M. J.; Summers, S. A.; Scherer, P. E. Receptor-mediated activation of ceramidase activity initiates the pleiotropic actions of adiponectin. *Nat. Med.* **2011**, *17* (1), 55–63.

(38) Villa, N. Y.; Kupchak, B. R.; Garitaonandia, I.; Smith, J. L.; Alonso, E.; Alford, C.; Cowart, L. A.; Hannun, Y. A.; Lyons, T. J. Sphingolipids function as downstream effectors of a fungal PAQR. *Mol. Pharmacol.* **2009**, *75* (4), 866–75.

(39) Maines, M. D.; Gibbs, P. E. 30 some years of heme oxygenase: from a “molecular wrecking ball” to a “mesmerizing” trigger of cellular events. *Biochem. Biophys. Res. Commun.* **2005**, *338* (1), 568–77.

(40) Li, M.; Kim, D. H.; Tsenovoy, P. L.; Peterson, S. J.; Rezzani, R.; Rodella, L. F.; Aronow, W. S.; Ikehara, S.; Abraham, N. G. Treatment of obese diabetic mice with a heme oxygenase inducer reduces visceral and subcutaneous adiposity, increases adiponectin levels, and improves insulin sensitivity and glucose tolerance. *Diabetes* **2008**, *57* (6), 1526–35.

(41) Bourquard, N.; Ng, C. J.; Reddy, S. T. Impaired hepatic insulin signaling in PON2 deficient mice - a novel role for the PON2/ApoE axis on macrophage inflammatory response. *Biochem. J.* **2011**, *436* (1), 91–100.

(42) Yang, M.; Zhang, Y.; Pan, J.; Sun, J.; Liu, J.; Libby, P.; Sukhova, G. K.; Doria, A.; Katunuma, N.; Peroni, O. D.; Guerre-Millo, M.; Kahn, B. B.; Clement, K.; Shi, G. P. Cathepsin L activity controls adipogenesis and glucose tolerance. *Nat. Cell Biol.* **2007**, *9* (8), 970–7.

(43) Lafarge, J. C.; Naour, N.; Clement, K.; Guerre-Millo, M. Cathepsins and cystatin C in atherosclerosis and obesity. *Biochimie* **2010**, *92* (11), 1580–6.

(44) Chun, T. H.; Inoue, M.; Morisaki, H.; Yamanaka, I.; Miyamoto, Y.; Okamura, T.; Sato-Kusubata, K.; Weiss, S. J. Genetic link between obesity and MMP14-dependent adipogenic collagen turnover. *Diabetes* **2010**, *59* (10), 2484–94.

(45) Khan, T.; Muise, E. S.; Iyengar, P.; Wang, Z. V.; Chandalia, M.; Abate, N.; Zhang, B. B.; Bonaldo, P.; Chua, S.; Scherer, P. E. Metabolic dysregulation and adipose tissue fibrosis: role of collagen VI. *Mol. Cell Biol.* **2009**, *29* (6), 1575–91.

(46) Nakamura, N.; Tanaka, S.; Teko, Y.; Mitsui, K.; Kanazawa, H. Four Na<sup>+</sup>/H<sup>+</sup> exchanger isoforms are distributed to Golgi and post-Golgi compartments and are involved in organelle pH regulation. *J. Biol. Chem.* **2005**, *280* (2), 1561–72.

(47) Pouyssegur, J.; Franchi, A.; L'Allemain, G.; Paris, S. Cytoplasmic pH, a key determinant of growth factor-induced DNA synthesis in quiescent fibroblasts. *FEBS Lett.* **1985**, *190* (1), 115–9.

(48) Yang, J.; Gillingham, A. K.; Hodel, A.; Koumanov, F.; Woodward, B.; Holman, G. D. Insulin-stimulated cytosol alkalization facilitates optimal activation of glucose transport in cardiomyocytes. *Am. J. Physiol. Endocrinol. Metab.* **2002**, *283* (6), E1299–307.

(49) Meima, M. E.; Webb, B. A.; Witkowska, H. E.; Barber, D. L. The sodium-hydrogen exchanger NHE1 is an Akt substrate necessary for actin filament reorganization by growth factors. *J. Biol. Chem.* **2009**, *284* (39), 26666–75.

(50) Lee-Kwon, W.; Johns, D. C.; Cha, B.; Cavet, M.; Park, J.; Tschlis, P.; Donowitz, M. Constitutively active phosphatidylinositol 3-kinase and AKT are sufficient to stimulate the epithelial Na<sup>+</sup>/H<sup>+</sup> exchanger 3. *J. Biol. Chem.* **2001**, *276* (33), 31296–304.

(51) Lawrence, S. P.; Holman, G. D.; Koumanov, F. Translocation of the Na<sup>+</sup>/H<sup>+</sup> exchanger 1 (NHE1) in cardiomyocyte responses to insulin and energy-status signalling. *Biochem. J.* **2010**, *432* (3), 515–23.

(52) Lebiezinska, M.; Szabadkai, G.; Jones, A. W.; Duszynski, J.; Wieckowski, M. R. Interactions between the endoplasmic reticulum, mitochondria, plasma membrane and other subcellular organelles. *Int. J. Biochem. Cell Biol.* **2009**, *41* (10), 1805–16.

(53) Levine, T.; Loewen, C. Inter-organelle membrane contact sites: through a glass, darkly. *Curr. Opin. Cell Biol.* **2006**, *18* (4), 371–8.

(54) Pichler, H.; Gaigg, B.; Hrastnik, C.; Achleitner, G.; Kohlwein, S. D.; Zellnig, G.; Perktold, A.; Daum, G. A subfraction of the yeast endoplasmic reticulum associates with the plasma membrane and has a high capacity to synthesize lipids. *Eur. J. Biochem.* **2001**, *268* (8), 2351–61.

(55) Koziel, K.; Lebiezinska, M.; Szabadkai, G.; Onopiuk, M.; Brutkowski, W.; Wierzbicka, K.; Wilczynski, G.; Pinton, P.; Duszynski, J.; Zablocki, K.; Wieckowski, M. R. Plasma membrane associated membranes (PAM) from Jurkat cells contain STIM1 protein is PAM involved in the capacitative calcium entry? *Int. J. Biochem. Cell Biol.* **2009**, *41* (12), 2440–9.